

Extended Binding Site on Fibronectin for the Functional Upstream Domain of Protein F1 of *Streptococcus pyogenes*^{*[S]}

Received for publication, June 17, 2010, and in revised form, September 23, 2010 Published, JBC Papers in Press, October 13, 2010, DOI 10.1074/jbc.M110.153622

Lisa M. Maurer¹, Bianca R. Tomasini-Johansson, Wenjiang Ma, Douglas S. Annis, Nathan L. Eickstaedt, Martin G. Ensenberger, Kenneth A. Satyshur, and Deane F. Mosher²

From the Departments of Biomolecular Chemistry and Medicine, University of Wisconsin, Madison, Wisconsin 53706

The 49-residue functional upstream domain (FUD) of *Streptococcus pyogenes* F1 adhesin interacts with fibronectin (FN) in a heretofore unknown manner that prevents assembly of a FN matrix. Biotinylated FUD (b-FUD) bound to adsorbed FN or its recombinant N-terminal 70-kDa fibrin- and gelatin-binding fragment (70K). Binding was blocked by FN or 70K, but not by fibrin- or gelatin-binding subfragments of 70K. Isothermal titration calorimetry showed that FUD binds with K_d values of 5.2 and 59 nM to soluble 70K and FN, respectively. We tested sets of FUD mutants and epitope-mapped monoclonal antibodies (mAbs) for ability to compete with b-FUD for binding to FN or to block FN assembly by cultured fibroblasts. Deletions or alanine substitutions throughout FUD caused loss of both activities. mAb 4D1 to the ²FNI module had little effect, whereas mAb 7D5 to the ⁴FNI module in the fibrin-binding region, 5C3 to the ⁹FNI module in the gelatin-binding region, or L8 to the G-strand of ¹FNI module adjacent to ⁹FNI caused loss of binding of b-FUD to FN and decreased FN assembly. Conversely, FUD blocked binding of 7D5, 5C3, or L8, but not of 4D1, to FN. Circular dichroism indicated that FUD binds to 70K by β -strand addition, a possibility supported by modeling based on crystal structures of peptides bound to ²FNI-⁵FNI of the fibrin-binding domain and ⁸FNI-⁹FNI of the gelatin-binding domain. Thus, the interaction likely involves an extensive anti-parallel β -zipper in which FUD interacts with the E-strands of ²FNI-⁵FNI and ⁸FNI-⁹FNI.

The blood plasma and extracellular matrix glycoprotein fibronectin (FN)³ is important in embryogenesis and development (1, 2) and in pathophysiology, e.g. after ischemic brain injury (3) or in platelet thrombus formation (4, 5). One means by which FN contributes to these processes is through the formation of insoluble fibrils, a process known as FN assembly (6, 7). FN assembly is a cell-mediated process that requires

the N-terminal 70-kDa region (70K) in the initial interaction between FN and the cell surface (8). 70K contains nine type I (FNI) modules and two type II (FNII) modules (Fig. 1A). FNI modules are composed of ~45 amino acids and contain a major β -sheet (C-, D-, and E-strands), a minor β -sheet (A- and B-strands), and two conserved disulfide bonds (9). FNI modules are rare and only found in chordates (10). In vertebrates, besides the 12 FNI modules in FN, there are single FNI modules in hepatocyte growth factor-activating protease, tissue plasminogen activator, and FXII (11). Thus, tandem FNI modules are a unique feature of FN.

The importance of 70K in FN assembly was demonstrated in studies showing that 70K as a proteolytic fragment binds to the surface of fibroblasts or platelets with the same affinity and location as full-length FN (12–14). 70K thereby serves as a dominant negative inhibitor of assembly of exogenous FN into fibrils (12, 15, 16). The 27-kDa (27K, N-⁵FNI) fibrin-binding and 40-kDa (40K, ⁶FNI-⁹FNI) gelatin-binding subfragments of 70K are much less potent inhibitors of FN assembly than 70K (12). 70K missing individual FNI modules or blocks of FNI modules also binds less well to cells (17). Thus, binding of 70K to the cell surface requires multiple FNI modules. The cell surface molecules mediating the interaction between the tandem FNI modules of 70K with fibroblasts or platelets are not known.

Functional upstream domain (FUD), a 49-amino acid peptide from the F1 adhesin (or SfbI, the allelic variant) in *Streptococcus pyogenes*, binds to 70K, including both the fibrin- and gelatin-binding domains, and blocks FN assembly (18, 19). The F1 adhesin and its SfbI allelic variant from which FUD is derived are FN-binding proteins (FNBP) in a family known as microbial surface components recognizing adhesive matrix molecules (20, 21). FUD includes an N-terminal nonrepetitive sequence, which is thought to interact with the gelatin-binding domain, and a single FN binding repeat (FNBR) at the C terminus (Fig. 1B) (21, 22). Nonrepetitive sequences similar to that in FUD are also found in *Streptococcus equisimilis* and *Borrelia burgdorferi* (21). FNBRs are found in many FN-binding members of the microbial surface components recognizing the adhesive matrix molecule family (20, 21, 23) and are unstructured but become organized after binding to FN (24, 25). Using isothermal titration calorimetry (ITC), it was shown that peptides based on the FNBRs in SfbI bind to ¹FNI-⁵FNI or ²FNI-⁵FNI (26). Furthermore, NMR spectroscopy showed that these peptides bind to tandem FNI modules by a distinctive interaction with the E-strands of ²FNI-³FNI or ⁴FNI-⁵FNI in an anti-parallel β -sheet (26). This type of inter-

* This work was supported, in whole or in part, by National Institutes of Health Grant HL021644 (to D. F. M.).

⌘ Author's Choice—Final version full access.

[S] The on-line version of this article (available at <http://www.jbc.org>) contains supplemental Figs. 1 and 2.

¹ Supported by American Heart Association Grant 0815362G.

² To whom correspondence should be addressed: 1300 University Ave., Rm. 4285, Madison, WI 53706. Fax: 608-263-4969; E-mail: dfm1@medicine.wisc.edu.

³ The abbreviations used are: FN, fibronectin; FNI, FN type I module; FNII, FN type II module; FUD, functional upstream domain; FNBP, fibronectin-binding protein; FNBR, fibronectin binding repeat; ITC, isothermal titration calorimetry; b-FUD, biotinylated FUD; ELISA, enzyme-linked immunosorbent assay; FNIII, FN type III module.

FUD Interactions with the N Terminus of Fibronectin

action, known as the β -zipper, was first recognized in NMR studies of FNBR-derived peptides from the *Streptococcus dysgalactiae* FNBP bound to ¹FNI-²FNII (27). It appears to be a common mechanism of interaction for FNBPs, including those not in Gram-positive cocci, as well as unstructured proteins lacking FNBRs, including the Leptospiral Immunoglobulin-like protein B from *Leptospira interrogans* (28–31).

Here, we have used FUD mutants, epitope-mapped anti-FN monoclonal antibodies (mAbs), and physical techniques to define the binding interaction between FUD and FN. Mutagenesis studies indicated that the binding site for FN extends throughout FUD and that spacing and sequencing of FUD residues are essential. Studies of various FN constructs demonstrated tighter binding of FUD to 70K than to intact FN and implicated both the fibrin- and gelatin-binding domains of 70K. Locations of epitopes of mAbs that influenced the interaction of FUD with FN extend from ²FNI to ¹FNIII. Circular dichroism (CD) and homology modeling supported the possibility that C-terminal residues of FUD interact with ²FNI-⁵FNI and N-terminal residues of FUD can interact with ⁸FNI and ⁹FNI via β -strand addition. The FUD mutants and mAbs that blocked binding of FUD to FN also blocked FN assembly by cultured fibroblasts, suggesting that cell surface molecules on cells may interact with the N terminus of FN via the same paradigm as FUD.

EXPERIMENTAL PROCEDURES

Plasma FNs and 70K Fragment—Human plasma FN was prepared by heat precipitation and anion exchange chromatography of a fibrinogen-rich fraction as described previously (32). Plasma FN of rat, cow, and mouse was purified from plasma by gelatin affinity chromatography. Proteolytic 70K (Fig. 1A) was prepared as described previously (12).

Expression of FN Modules Using pAcGP67.coco (COCO)—cDNA encoding rat FN was described previously (9, 17). The rat cDNA was used as template for PCR to create rat 70K and the following mutants: rat 70K K108R, rat 70K N221S, and rat 70K R567G. Primers specific for rat FN were used to introduce restrictions sites for cloning into the baculovirus expression vector pAcGP67.coco (33). The expressed protein begins at residue Gln-33, which is the start of the mature protein after the pre-prosequence, and ends at residue Pro-606. The human sequence begins at the same relative position, but the numbering (Gln-32) is off by one through residue 275 in comparing human with rat FN because in rat compared with human FN there is an extra residue in the pre-prosequence that is compensated for by absence of one residue in the linker between ⁵FNI and ⁶FNI of the rat protein. Mutated rat residues are numbered according to the rat sequence.

A schematic of human FN constructs is shown in Fig. 1A. Recombinant 70K (N-⁹FNI, residues 32–608), N-⁵FNI (residues 32–290), N-³FNI (residues 32–183), ⁴FNI-⁵FNI (residues 184 to 290), ⁶FNI-⁹FNI (residues 291–608), ⁷FNI-⁹FNI (residues 468–608), and N-³FNIII and N-³FNIII Q690R (residues 32–904) were expressed as secreted His-tagged proteins using the baculovirus vector pAcGP67.coco (COCO) (8, 33). Expression and purification of ¹FNIII-C EDA⁺ (V89) were described previously (34). The His-tagged recombinant proteins

were purified by Ni²⁺-chelate chromatography. Recombinant human and rat 70K, rat 70K mutants, and N-⁵FNI were dialyzed into 10 mM Tris, 300 mM NaCl, 1 M NaBr, pH 7.4. ⁶FNI-⁹FNI and ⁷FNI-⁹FNI were dialyzed into Tris-buffered saline (TBS, 10 mM Tris, 150 mM NaCl, pH 7.4). ¹FNIII-C EDA⁺ (V89) was dialyzed into 10 mM MOPS, 300 mM NaCl, pH 7.4. All other constructs were dialyzed into 10 mM Tris, 300 mM NaCl, pH 7.4. Concentration was determined using extinction coefficients at 280 nm as predicted from amino acid composition using Protogram at the ExPASy website.

Monoclonal Antibodies (mAb)—The murine mAbs 7D5, 4D1, and 5C3 were selected from a panel of mAbs generated against recombinant human 70K. These antibodies were produced in collaboration with Dr. MaryAnn Accavitti-Loper and the University of Alabama-Birmingham Epitope Recognition and Immunoreagent Core Facility. Polyclonal rabbit antibodies were raised using the cathepsin D 70K fragment of human FN (35). L8 was described previously (36).

Cloning and Expression of FUD Proteins—Because we encountered instability with pELMER previously used to express FUD (37), recombinant FUD constructs were expressed in pET-28c⁺ (EMD, Gibbstown, NJ) that was modified to contain a piece of the multiple cloning site of pELMER. Thus, a segment of pELMER that encoded the N-terminal His₆ tag followed by a thrombin cleavage site along with the multiple cloning site was inserted into pET-28c⁺ to create pET-ELMER. Mutations were introduced into FUD in pELMER using PCR-based strategies, and the mutated DNA was then inserted into pET-ELMER. The presence of correct sequences was confirmed.

Constructs in pET-ELMER were transformed into BL21(DE3) cells (EMD) for expression and induced with 1 mM isopropyl β -D-1-thiogalactopyranoside. Bacteria were lysed in lysis buffer with or without urea. The cleared lysate was incubated overnight with nickel-nitrilotriacetic acid agarose (Qiagen), washed, and eluted with elution buffer (100 mM NaH₂PO₄, 10 mM Tris, 8 M urea, 250 mM imidazole, pH 8.0). The His tag was removed as described previously (37) except that 1 unit of biotinylated thrombin per mg of protein was added for 2 h. Proteins were further purified via fast protein liquid chromatography (GE Healthcare) using a High-Trap Mono Q column. To do this, proteins were dialyzed into 20 mM Tris, 20 mM NaCl, pH 7.4, and eluted via a NaCl gradient from 20 to 300 mM. Most proteins eluted at ~100 mM NaCl. Proteins that eluted outside the range of 80–120 mM NaCl were dialyzed into 20 mM Tris, 100 mM NaCl, pH 7.4. The sequence of FUD is given in Fig. 1C. It should be noted that the protein is 56 rather than 49 residues in length with N- and C-terminal “tails” of 5 and 2 residues, respectively, introduced by the expression strategy (Fig. 1C). The quality of the constructs was assessed by SDS-PAGE and matrix-assisted laser desorption/ionization time-of-flight mass spectrometry. All were pure on an overloaded gel and homogeneous and were of the expected mass as shown by mass spectrometry (data not shown). Concentrations were determined using extinction coefficients at 280 nm for cleaved proteins, which were calculated using Protogram from ExPASy.

Labeling of FN and Biotinylation of FUD—Fluorescein isothiocyanate FN (FITC-FN) was made as described previously

(12). FUD was dialyzed into phosphate-buffered saline (PBS, 8 mM Na₂HPO₄, 137 mM NaCl, 1.76 mM KH₂PO₄, 2.7 mM KCl, pH 7.4), and *N*-hydroxysulfosuccinimide-biotin (Pierce) at 20-fold molar excess of FUD was added at room temperature for 1 h after which unincorporated biotin was removed by dialysis into PBS followed by 20 mM Tris, 100 mM NaCl, pH 7.4.

Cell Culture and Fluorescence Microscopy—FN^{-/-} mouse fibroblasts were derived from stem cells of FN knock-out mice (1) as described previously (38). Cells were cultured in Dulbecco's modified Eagle's medium (DMEM, Invitrogen) with 10% fetal bovine serum (Intergen, Purchase, NY), 100 IU/ml penicillin, and 100 mg/ml streptomycin.

Coverslips were coated with 15 μg/ml laminin. FN^{-/-} cells were plated 3 h prior to addition of 20 nM FITC-FN and 50 or 500 nM FUD, FUD mutants, 40 μg/ml mAbs, or control mouse IgG (Pharmingen) in DMEM plus 0.2% bovine serum albumin (BSA). Following a 45-min incubation, cells were washed once and fixed with 3.7% paraformaldehyde in PBS, washed, and mounted on slides using Immuno-mount (Thermo Scientific, Pittsburgh, PA) as described previously (8). Cells were viewed on an Olympus epifluorescence microscope, and representative fields were digitally photographed using the same exposure time as optimized for cells not treated with FUDs or mAbs.

Binding Assays with FUD—Enzyme-linked assays were done using high binding plates (Corning 3590) coated overnight at 4 °C with 50 μl of 10 μg/ml (40 nM) human or rat FN, 2.7 μg/ml (40 nM) 70K, or 7.7 μg/ml (40 nM) ¹FNIII-C EDA⁺, or human or rat recombinant constructs (10 μg/ml) with mutations described above. Plates were blocked with 5% BSA in TBS containing 0.05% Tween 20 (TBST). For the experiment looking at binding of biotinylated-FUD (b-FUD), increasing concentrations of b-FUD were incubated on the plate for 2 h in TBST containing 0.1% BSA. For competition of b-FUD binding, 0.3 nM b-FUD was added to wells simultaneously with the indicated concentration of FN or FN construct; unlabeled FUD or FUD mutant; or purified 4D1, 7D5, or 5C3; or 1 mM ZnSO₄ in TBST containing 0.1% BSA for 2 h. Plates were washed and incubated with a 1:20,000 dilution of alkaline phosphatase-conjugated streptavidin (Jackson ImmunoResearch, West Grove, PA) for 1 h. For experiments examining the effects of increasing concentrations of FUD or d29 or mAb binding, 1:50,000 dilution of 4D1 or 7D5 ascites, a 1:30,000 dilution of 5C3 ascites, or 0.1 μg/ml purified L8 IgG was added to wells simultaneously with increasing concentrations of FUD or d29 in TBST containing 0.1% BSA for 2 h. Plates were washed and incubated with 1:5000 dilution of alkaline phosphatase donkey α-mouse secondary (Jackson ImmunoResearch) for 1 h. 4-Nitrophenyl phosphate disodium salt hexahydrate was used at 1 mg/ml in TBS, pH 9.0 (Sigma). Some assays were stopped with an equal volume of 3 N NaOH. Absorbance at 405 nm was determined using a Tecan Genios Pro (Tecan, Durham, NC) microplate reader. All conditions were tested in triplicate and compared with antibody alone or b-FUD alone after background subtraction. Unless indicated otherwise, the graphs are means ± S.D. of the means of triplicates from three to four separate experiments.

ITC—ITC was carried out with a VP-ITC microcalorimeter (MicroCal, LLC) at 25 °C. The cell had a volume of 2.2 ml. In a typical experiment, the cell contained 1.4 ml of a solution of FN or 70K, and the syringe contained 1 ml of FUD. The titration was performed in 37 injections (1 × 1, 4 × 4, and 32 × 8 μl) delivered at 120-s intervals into the protein solution. The initial data point was routinely discarded. The concentrations of FUD, FN, and 70K are described in Table 1. The interaction of FUD-FN was in PBS buffer, pH 7.4, and the interaction of FUD-70K was in 25 mM sodium phosphate buffer, pH 7.2. Data were fit by Lavenberg-Marquardt nonlinear regression with Origin 7.0 using the one-site model.

CD—CD analysis was performed on an AVIV stopped flow CD spectrometer under N₂ atmosphere. Five spectra were obtained at 25 °C in 0.1-cm path length cells and from 190 to 280 nm for far-UV CD for each condition. Heat denaturation of 70K or FUD was done by measuring the ellipticity after heating the jacketed cells to 40, 60, and 80 °C at 5 °C/min. Spectra were recorded in 25 mM sodium phosphate buffer, pH 7.0. Spectra of 1 μM FUD, 70K, or 1:1 FUD-70K complex were obtained at 25 °C. Changes due to formation of the FUD-70K complex were explored by comparison of the sum of the spectra of FUD and 70K to the spectrum of the complex and by subtraction of the spectrum of 70K from the spectrum of the complex. In the latter case, the spectrum of FUD and the difference spectrum were also expressed as mean residue ellipticity in units of degrees cm² dmol⁻¹ of FUD, assuming that all of the difference was due to a change in the conformation of FUD upon complex formation. In CD experiments, the background spectrum of buffer without protein is subtracted from the protein spectrum.

Western Blotting—Western blots were performed as described previously (39). Approximate molar equivalents (5 pmol) of human 70K, rat 70K, or rat 70K mutant proteins were resolved on 8% SDS-polyacrylamide gels. Proteins were detected with mAbs 4D1, 7D5, 5C3, and L8 or polyclonal antibody raised against human 70K.

Direct Enzyme-linked Immunosorbent Assay (ELISA)—Antigen diluted to 10 μg/ml in TBS or, for chicken FN, plasma diluted 1:10 was used to coat 96-well microtiter plates (Costar 3590, Corning Inc., Corning, NY), where blocking, washing, and antibody addition were carried out as described previously (39). The appropriate species-specific horseradish peroxidase-conjugated secondary antibody was incubated with the plate for 1 h. After washing four times with TBST, 50 μl per well of SureBlue TMB peroxidase substrate (Kirkegaard & Perry Laboratories, Gaithersburg, MD) was added to each well. Color development was monitored, and after a 5–30-min incubation, 50 μl per well of TMB stop solution (Kirkegaard & Perry Laboratories) was added followed by measurement of absorbance at 450 nm.

Homology Modeling—For homology modeling, we used Protein Data Bank structures of the C-terminal STATT-5 peptide from the fifth FNBR of *Staphylococcus aureus* FN-binding protein A (FNBP A) bound to ²FNI-³FNI (Protein Data Bank code 3CAL), the N-terminal STAFF-5 peptide from FNBR-5 of FNBP A bound to ⁴FNI-⁵FNI (Protein Data Bank code 2RLO) (28), and a peptide from the α1(I) chain of

FUD Interactions with the N Terminus of Fibronectin

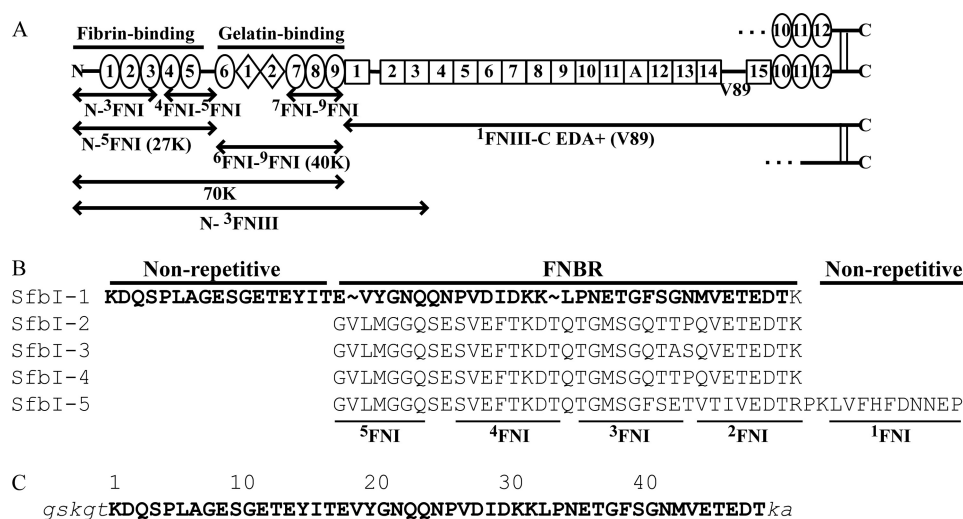


FIGURE 1. Diagrams of FN and FN fragments, the FN-binding region of the F1 adhesin of *S. pyogenes*, and sequence of recombinant FUD. A, each subunit of FN consists of 12 FNI modules (ovals), 2 FNII modules (diamonds), and 16 FNIII modules (squares) for the EDA⁺, V89 splice variant shown. In plasma FN, one subunit contains a variable region, and the other subunit lacks it. Modules are numbered to facilitate naming recombinant proteins according to modular content. Proteolytic fragments are named by size. B, five FNBRs and the N- and C-terminal nonrepetitive sequences of SfbI. Sequences that were predicted to interact with FNI modules in the studies of Schwarz-Linek *et al.* (21) are underlined. FUD, which includes the N-terminal nonrepetitive sequence and most of the SfbI-1 FNBR, is in boldface. C, sequence of expressed FUD with tails in lowercase and italics and the 49-residue FUD sequence in uppercase and boldface. Residues of FUD *per se* are numbered.

type I collagen bound to ⁸FNI-⁹FNI (Protein Data Bank code 3EJH) (40). Using Sybyl modeling software (Tripos Corp., St. Louis), we built FUD in place of FNBP-5 or collagen peptide and energy-minimized the resulting structures. Because the collagen peptide did not extend completely through ⁹FNI, to model the interaction between FUD and ⁹FNI, we copied the peptide bound to ⁸FNI, placed it on ⁹FNI, and substituted residues as with other modules. Side chains were manually torsioned to relieve clashes with the backbone fixed. After addition of hydrogens and Gasteiger-Hückel charges, energy minimization was performed using the Tripos force field in Sybyl, first using the Simplex minimization, followed by the Powell conjugate gradient minimization (41). Additional modeling was done of various 6-residue peptides bound to individual FNI modules. Minimization was terminated when the gradient of change was less than 0.05 kcal/(mol·Å).

RESULTS

FUD Binds to Soluble 70K with a Higher Affinity than Soluble FN—To understand better the interaction between FUD and FN, we utilized monomeric recombinant FUD with short N- and C-terminal tails (Fig. 1C). This construct contains the unique upstream sequence plus the first FNBR of the F1 adhesin (SfbI) (Fig. 1B). Because of vector instability with the previously used pELMER vector that allowed expression of such a monomeric protein (37), we modified pET-28c⁺ to include a thrombin cleavage site after the N-terminal His-tag as in pELMER. FUD and FUD mutants were cleaved with thrombin and purified via fast protein liquid chromatography. The material was highly pure by SDS-PAGE and contained a single species of the correct mass as accessed by mass spectrometry.

We used an enzyme-linked assay to quantify the ability of b-FUD to bind to surfaces coated with dimeric FN, monomeric 70K, or dimeric ¹FNIII-C EDA⁺ that lacked the 70K N-terminal regions. b-FUD bound to FN and 70K, but not

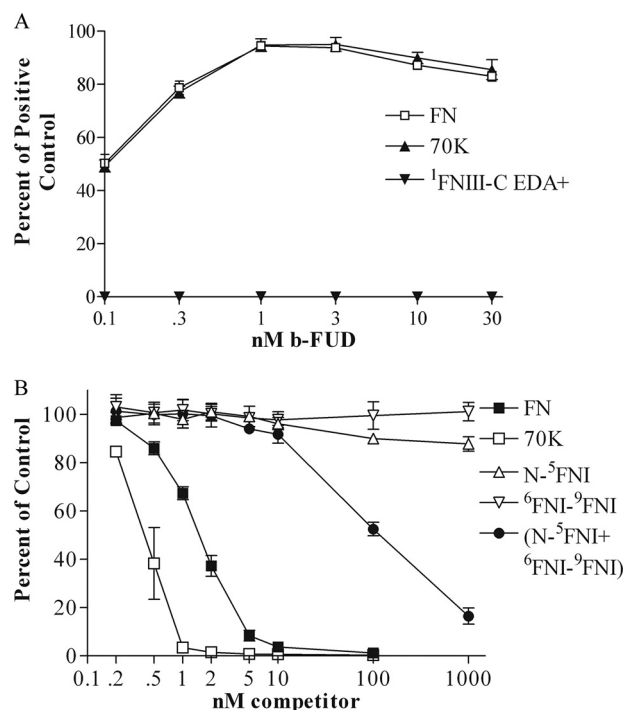


FIGURE 2. b-FUD binds to FN and 70K. A, enzyme-linked assay of binding of increasing concentrations of b-FUD binding to coated FN (□), 70K (▲), or ¹FNIII-C EDA⁺ (▼). The amount bound was compared with a positive control signal of wells coated with b-FUD at 1 μg/ml. Values are means ± S.D. of one or three experiments. B, binding relative to no competitor of 0.3 nM b-FUD binding to 10 μg/ml adsorbed FN with increasing concentrations of FN proteins. FN proteins are as follows: full-length FN (■), 70K (□), N-⁵FNI (△), ⁶FNI-⁹FNI (▽), N-⁵FNI plus ⁹FNI-⁹FNI (●). Values are means ± S.D. of three experiments.

¹FNIII-C EDA⁺, as expected (18), showing that binding to FN is to the 70K region (Fig. 2A).

To test whether binding of b-FUD to adsorbed FN or 70K is the same as binding of b-FUD to the soluble proteins, we

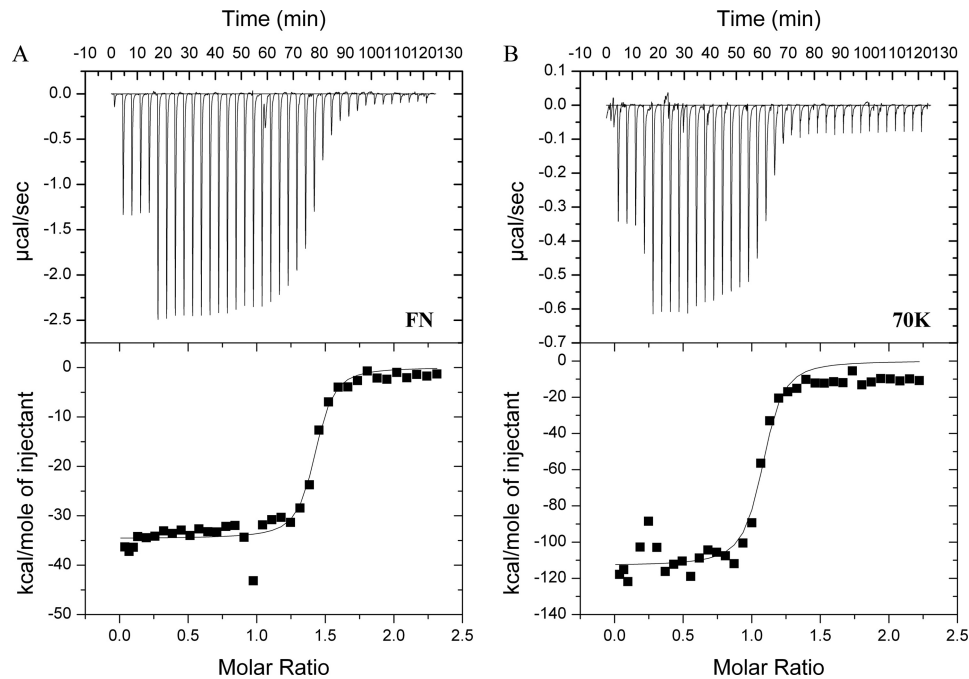


FIGURE 3. **FUD has a higher affinity for 70K than for FN.** ITC of interaction of FUD with FN (A) or 70K (B). Raw titration data and integrated heat with experimental data (dot) and best fit (line) are shown in the top and bottom panels, respectively. Different volumes were injected during the course of the experiment (1×1 , 4×4 , and $32 \times 8 \mu\text{l}$). The concentrations of proteins and the thermodynamic parameters are shown in Table 1.

TABLE 1
ITC analysis of FUD binding to FN or 70K

K_d values and thermodynamic parameters for FUD binding to FN or 70K.

Interaction	[FUD]	[FN]/[70K]	ΔH	ΔS	ΔG	K_d	n
	μM	μM	kcal mol^{-1}	$\text{cal mol}^{-1} \text{K}^{-1}$	kcal mol^{-1}	nM	
FUD-FN	204	8.95	-29.9	-72	-9.9	59	1.7
FUD-70K	15.8	1.4	-44.3	-117	-11.3	5.2	1.1

compared the ability of unlabeled FN or 70K in solution to compete for binding of b-FUD to adsorbed FN. Preincubation of 1 nM 70K with 0.3 nM b-FUD caused nearly complete loss of b-FUD binding to FN-coated plates. Higher FN:FUD ratios were required to achieve similar inhibition of binding (Fig. 2B). We also examined the ability of recombinant N-⁵FNI or ⁶FNI-⁹FNI to compete with b-FUD for binding to FN. N-⁵FNI competed with b-FUD to a minor degree at 1000 nM. A mixture of N-⁵FNI and ⁶FNI-⁹FNI competed with b-FUD better than each alone, but with greater than 100-fold decreased activity as compared with intact 70K (Fig. 2B). These results reveal that soluble 70K binds FUD more tightly than FN and such binding requires the presence of both the fibrin- and gelatin-binding domains.

To corroborate the finding from competition assays that FUD binds more tightly to 70K than FN, we performed ITC. The curves fit a model of two identical binding sites in dimeric FN (Fig. 3A and Table 1) and one binding site in monomeric 70K (Fig. 3B and Table 1). Binding constants of FUD-FN and FUD-70K and thermodynamic parameters for these bindings are in Table 1. Binding of FUD to FN was an exothermic reaction with a dissociation constant (K_d) of 59 nM. The binding of FUD to 70K was also an exothermic reaction with a K_d of 5.2 nM. This value is close to the 4 nM affinity, also measured by ITC, mentioned in a recent review (21).

Thus, the interaction between FUD and 70K has a 10-fold greater affinity than the interaction between FUD and FN as determined by ITC.

Effect of FUD Mutants on b-FUD Binding to FN and Matrix Assembly—A series of FUD mutants was made to determine sequence requirements for the binding of FUD to adsorbed FN as measured in a competition assay. We tested the importance of sequence and spacing with a series of deletions (d) as follows: d21–25, d27–31, d28–30, d29, d32–36, and d37–41; and the insertion of single alanine between Ile-29 and Asp-30 (i29/30) (Fig. 1C). At a concentration of 10 μM , FUD blocked all binding of 0.3 nM b-FUD to adsorbed FN (Fig. 4A). There was a 20% competition by 10 μM i29/30 for b-FUD binding to FN (Fig. 4A). All FUDs harboring deletions failed to compete with 0.3 nM b-FUD at concentrations of 10 μM (Fig. 4A).

We also tested a series of block alanine substitutions to localize residues in FUD that are important for FN binding. Wild type FUD blocked 0.3 nM b-FUD binding to FN significantly at 0.1 μM and completely at 1 μM (Fig. 4B). As concentrations increased from 0.01 to 10 μM , Ala-2–6, Ala-21–25, and Ala-29 also competed with 0.3 nM b-FUD for binding to FN. However, activities were lower than with FUD (Fig. 4B). Ala-7–11, Ala-12–16, Ala-17–20, Ala-27–31, Ala-37–41, and Ala-43–47 did not block the binding of 0.3 nM b-FUD to FN even at concentrations up to 10 μM (Fig. 4B). This finding

FUD Interactions with the N Terminus of Fibronectin

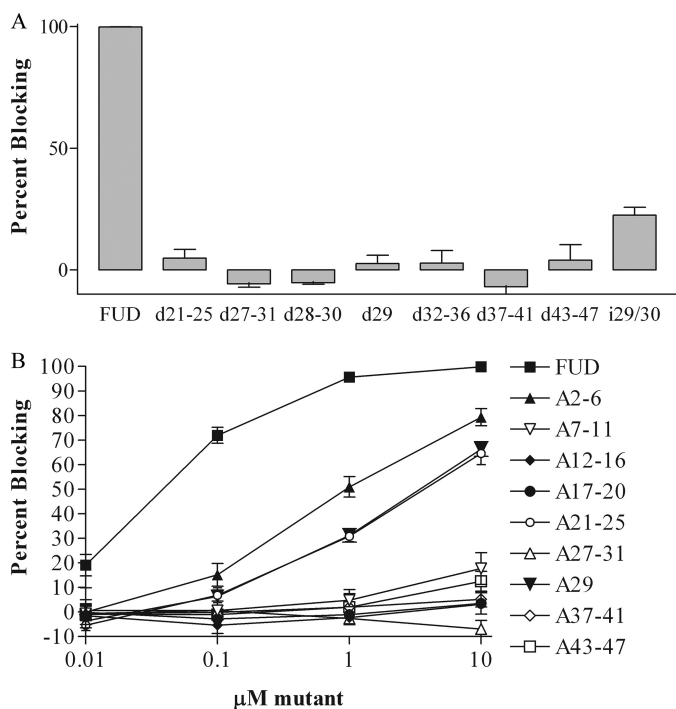


FIGURE 4. Spacing and sequence of FUD are important for binding of FUD to FN. *A*, effects of 10 μM FUD with deletion or insertion mutations on blocking 0.3 nM b-FUD from binding to coated FN. *B*, effect of alanine substitutions on the ability of increasing concentrations of FUD to block 0.3 nM b-FUD binding to coated FN. FUD constructs are as follows (where A is Ala): FUD (■), A2-6 (▲), A7-11 (▽), A12-16 (◆), A17-20 (●), A21-25 (○), A27-31 (△), A29 (▼), A37-41 (◇), A43-47 (□). Values are means \pm S.D. of three experiments.

suggests that there are residues that contribute importantly for binding to FN throughout FUD.

In parallel, we looked at the ability of FUD mutants to block the assembly of exogenous FN by cultured FN^{-/-} cells. At both 50 and 500 nM, FUD blocked the assembly of exogenous FITC-FN (Fig. 5). Addition of Ala-2-6 and Ala-21-25 at 500 nM also blocked the assembly of exogenous FITC-FN, but no effect was found where the concentration was reduced to 50 nM. Neither 500 nM d29 nor d21-25 affected the assembly of exogenous FITC-FN (Fig. 5). Other deletion mutants, i29/30, or the remainder of the alanine block substitution mutants did not block assembly of exogenous FITC-FN at a concentration of 500 nM (data not shown). Thus, the structure-function relationships within the set of the FUD mutants were identical for competition of binding of b-FUD to FN and for impairment of FN assembly by cells.

Epitope Mapping of mAbs and Effects of mAbs on FUD Binding—The competition experiments comparing 70K to the 70K subfragments indicate that binding sites for FUD are present in both the fibrin- and gelatin-binding regions of 70K such that both regions contribute to high affinity binding. To identify regions of FN that interact with FUD using a second experimental paradigm, we mapped the epitopes of three anti-70K mAbs, 4D1, 7D5, and 5C3, selected because of their reactivities with different regions of 70K. All three mAbs lost reactivity when 70K was reduced (data not shown), indicating that the epitopes require intact disulfides and tertiary structure. We localized 4D1 to N-³FNI, 7D5 to ⁴FNI-⁵FNI, and

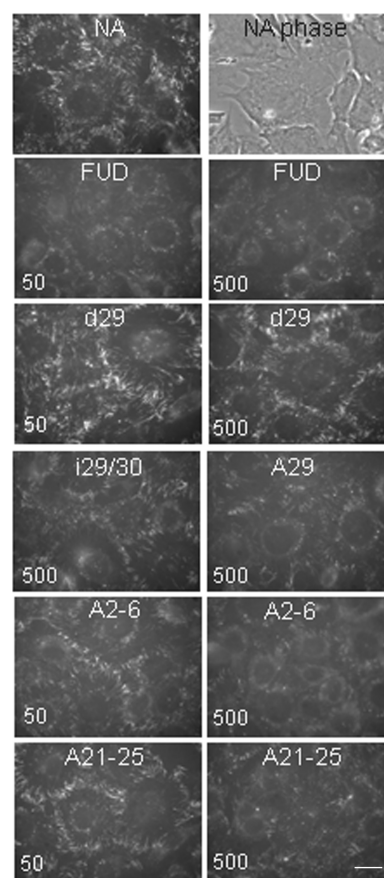


FIGURE 5. Effects of FUD mutants on FN assembly. FN^{-/-} cells adherent to laminin-coated coverslips were given 20 nM FITC-FN in the absence (NA) or presence of 50 or 500 nM FUD, d29, A2-6, or A21-25; or 500 nM i29/30 or A29. Following incubation for 45 min, cells were washed, fixed, and processed for fluorescence microscopy. All photomicrographs were taken at exposure time determined for NA control. Bar, 10 μm .

5C3 to ⁷FNI-⁹FNI using recombinant tandem modules (data not shown). We then determined whether the antibodies bound to mouse, rat, bovine, or chicken FN. Alignment of sequences from each species allowed predictions of residues that differ from human and thus have the potential to determine the epitopes (supplemental Fig. 1). Because none of the three antibodies bound to rat FN, we mutated the predicted residues in rat 70K to the residue found in human FN and expressed the rat 70K proteins using baculovirus. Each mAb and a polyclonal rabbit anti-human FN antibody were tested for reactivity to rat 70K proteins via ELISA and Western blot. mAb 4D1 bound human 70K and rat 70K K108R, but not rat 70K, rat 70K N221S, or rat 70K R567G (Fig. 6, A and B). This localizes 4D1 to the loop between the B- and C-strands of ²FNI (Fig. 6C). Likewise, 7D5 bound only human 70K and rat 70K N221S (Fig. 6, A and B). This localizes the epitope for 7D5 to the loop adjacent to the E-strand of ⁴FNI (Fig. 6C). mAb 5C3 bound human 70K and rat 70K R567G (Fig. 6, A and B). This localizes the epitope for 5C3 to the loop between the A- and B-strands of ⁹FNI (Fig. 6C). Polyclonal anti-FN antibodies bound to all human and rat 70K proteins but seemed to be directed mostly against epitopes determined by Gly-567 (Fig. 6B).

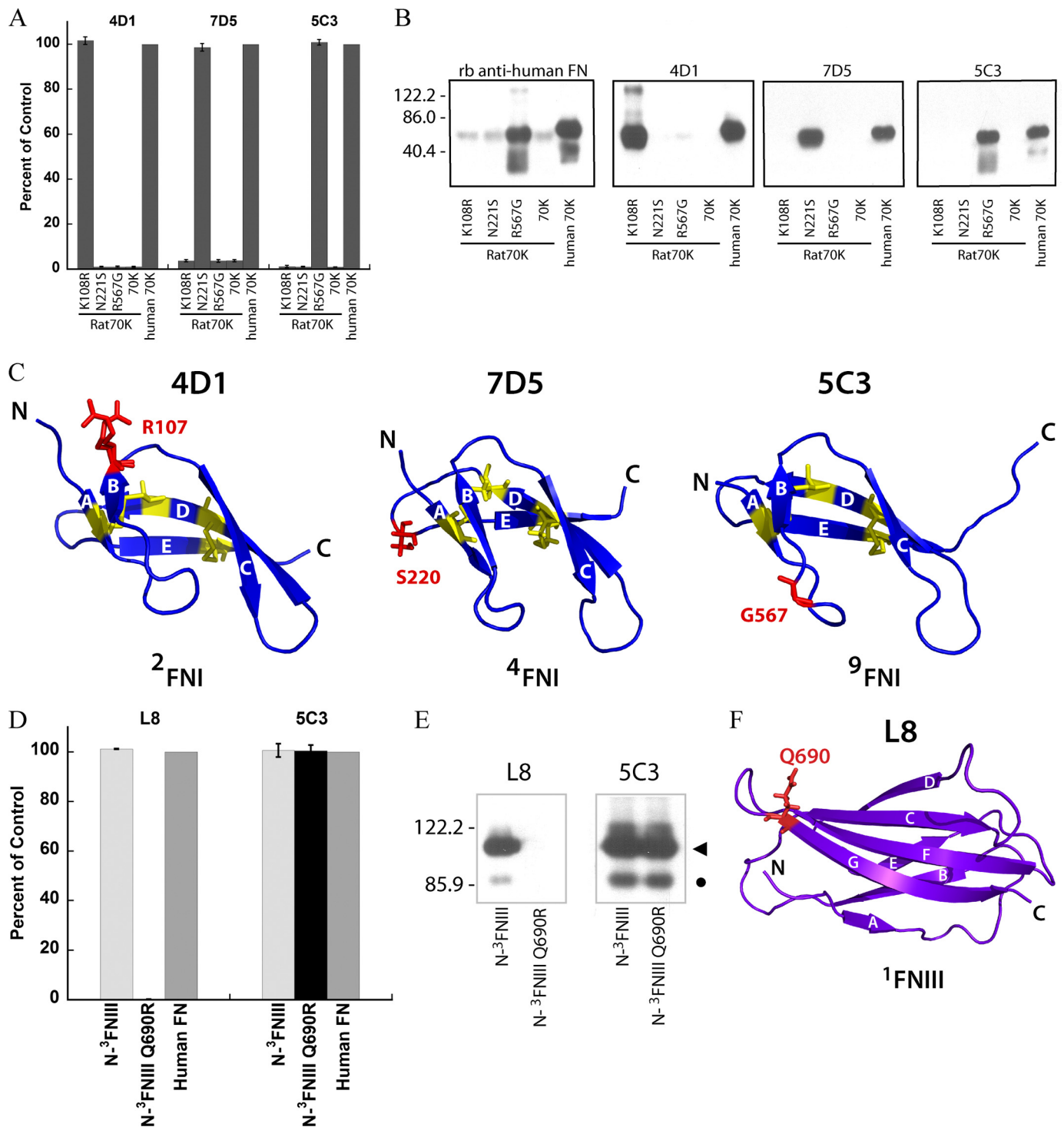


FIGURE 6. **Epitope mapping of mAbs.** *A*, ELISA results plotted as percent of human 70K control for recognition by 4D1, 7D5, or 5C3 with the three mutated rat 70K constructs and nonmutated rat 70K. *Error bars* represent standard deviation of four experiments. *B*, Western blots with a polyclonal rabbit (*rb*) anti-human 70K or the mAbs with the mutated rat 70K constructs, nonmutated rat 70K, and human 70K. *C*, structures of human FN modules ²FNI (47), ⁴FNI (54), and ⁹FNI (40) are shown with the residues that caused recovery of the epitopes in rat 70K in red (4D1, Arg-107; 7D5, Ser-220; 5C3, Gly-567). β-Strands (A–E) of the FNI modules are labeled. Disulfide-bonded cystines are in yellow. *D*, ELISA results plotted as percent of control (human FN) for L8 and 5C3 with human N-³FNIII and N-³FNIII Q690R. *Error bars* represent standard deviation of three experiments. *E*, Western blot of L8 and 5C3 with N-³FNIII, and N-³FNIII Q690R. The major 100-kDa band (▲), and a minor band (●), are indicated. *F*, structure of human FN module ¹FNIII (59) is shown with the predicted key residue Gln-690 for the L8 mAb epitope in red. β-Strands (A–G) of the ¹FNIII module are labeled.

The epitope for mAb L8 was also mapped because, although it does not recognize 70K, it recognizes proteins with the ⁹FNI-¹FNIII tandem (36). Recognition is lost when ⁹FNI is reduced or separated from ¹FNIII (36). As with the mAbs to

70K, L8 was tested for reactivity to mouse, rat, bovine, and chicken FN. The residue key for L8 recognition was predicted to be Gln-690 in ¹FNIII (supplemental Fig. 1). Because L8 reacts with both rat and human, but not murine FN, a strategy

FUD Interactions with the N Terminus of Fibronectin

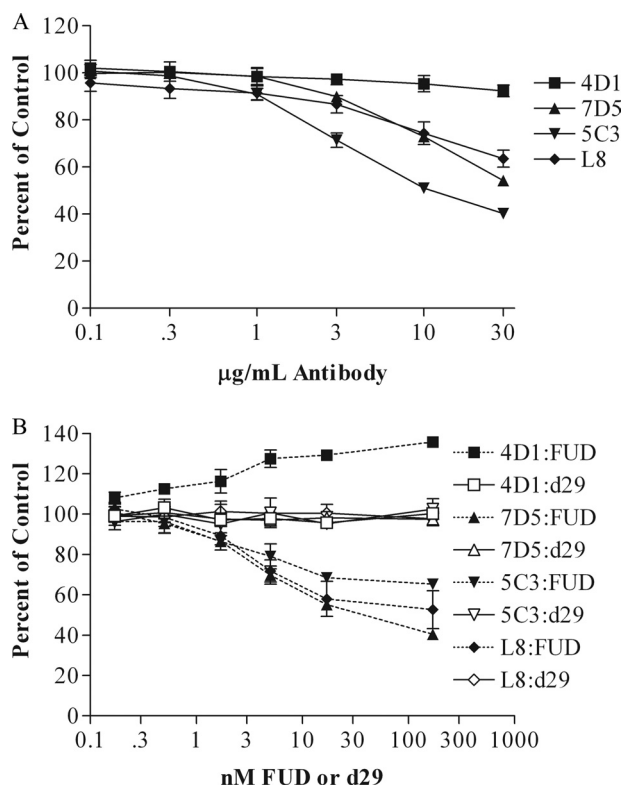


FIGURE 7. mAbs 7D5, 5C3, and L8 decrease FUD binding to FN and vice versa. A, binding relative to no mAb of 0.3 nM b-FUD to coated FN in the presence of increasing concentrations of purified mAbs. Antibodies are as follows: 4D1 (■), 7D5 (▲), 5C3 (▼), or L8 (◆). B, binding relative to no FUD of mAb to coated FN in the presence of increasing concentrations of FUD (solid symbols as above) or d29 (open symbols as above). Antibodies are as follows: 4D1 (1:50,000 ascites), 7D5 (1:50,000 ascites), 5C3 (1:30,000 ascites), and L8 (0.1 µg/ml). Values are means \pm S.D. of three experiments.

different from the one used to map the other mAbs was needed. The predicted epitope was targeted by mutating residue 690 in human N-³FNIII (see Fig. 1A) from glutamine to arginine as in mouse FN. L8 bound to N-³FNIII but not N-³FNIII Q690R in ELISA and Western blot (Fig. 6, D and E). This finding localizes the epitope for L8 to the start of the G-strand of ¹FNIII close to where ¹FNIII would be expected to abut ⁹FNI (Fig. 6F).

Increasing concentrations of 7D5, 5C3, or L8 decreased the binding of 0.3 nM b-FUD to FN (Fig. 7A). The decrease was greater than what was found with increasing concentration of mAb 4D1 (Fig. 7A). In the corollary experiment, increasing concentrations of FUD, but not d29, decreased the binding of 7D5, 5C3, and L8 to FN (Fig. 7B), whereas increasing the concentration of FUD, but not d29, increased rather than decreased binding of 4D1 to FN (Fig. 7B). These findings suggest that ²FNI, ⁴FNI, ⁹FNI, and ¹FNIII are all involved in the binding of FUD to adsorbed FN.

Control experiments were done to determine possible off target effects of the antibodies. Rat FN contains the epitope for L8, but not 4D1, 7D5, or 5C3. As would be expected, only L8 was able to block the binding of 0.3 nM b-FUD to rat FN (supplemental Fig. 2A). Also, as would be expected, 7D5 blocked b-FUD binding to rat 70K N221S but not rat 70K or rat 70K R567G (supplemental Fig. 2B). Likewise, 5C3 blocked

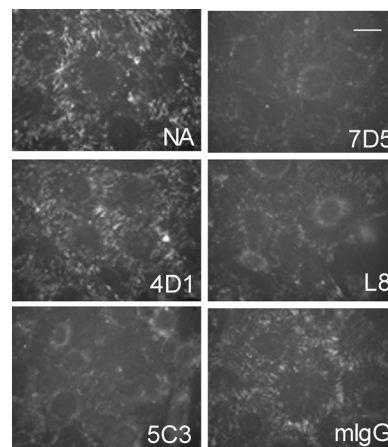


FIGURE 8. Effects of mAbs on FN matrix assembly. FN^{-/-} cells adhered onto laminin-coated coverslips were given 9 µg/ml FITC-FN in the absence (NA) or presence of 40 µg/ml 4D1, 5C3, 7D5, L8, or control mouse IgG. Following incubation for 45 min, cells were washed, fixed, and processed for fluorescence microscopy. Bar, 10 µm.

b-FUD binding to rat 70K R567G, but not rat 70K N221S or rat 70K (supplemental Fig. 2B).

Effects of mAbs on Matrix Assembly—To learn if the correlation between FUD binding and FN assembly holds true for the mAbs, we tested the ability of mAbs to block the assembly of exogenous FITC-FN by cultured FN^{-/-} fibroblasts. Addition of mAbs 7D5, 5C3, or L8 decreased the assembly of exogenous FITC-FN (Fig. 8). mAb 4D1 did not inhibit assembly of exogenous FITC-FN (Fig. 8).

Far-UV CD Spectrometry Studies of 70K, FUD, and 70K-FUD Complex—Far-UV CD was used to look for changes in secondary structure of FUD upon binding of FUD to 70K, as has been done for binding of other bacterial peptides to the fibrin-binding fragment (24, 25, 29). 70K had two positive bands, one at 227 nm and a second at 196 nm (Fig. 9A). The 227-nm band is likely due to aromatic residues sharing a similar stereochemical environment in the multiple FNI modules (42, 43), whereas the 196-nm band is compatible with β -sheet structure (44, 45). We assume that the strong positive band at 227 nm obscures a weak negative band at 215 nm, which is a feature of the signature spectrum of β -sheet. Upon heating, both 227- and 196-nm bands disappeared at 60 °C and above and were recovered incompletely upon cooling (data not shown). FUD had a negative band at 199 nm (Fig. 9A) that did not change upon heating (data not shown). Both the shape and intensity to heating are compatible with random coil (45). Comparing the spectrum of 70K-FUD 1:1 complex to the sum of the spectra of 70K and FUD (Fig. 9A), there was an increase of positive ellipticity at 196 nm rather than the decrease predicted by addition of the individual spectra. The increase must be due to new secondary structure, either α -helix or β -sheet (46). To explore this issue further, we assumed that the change is due solely to the FUD and compared the spectrum of FUD and the difference between the spectra of the FUD-70K complex and 70K alone, expressing both as decimoles of residues in FUD (Fig. 9B). Absence of the concomitant appearance of strong negative bands at 220 and 208 nm suggests that the new secondary structure is not α -helix and instead is β -sheet. The decimolar ellipticities of the negative

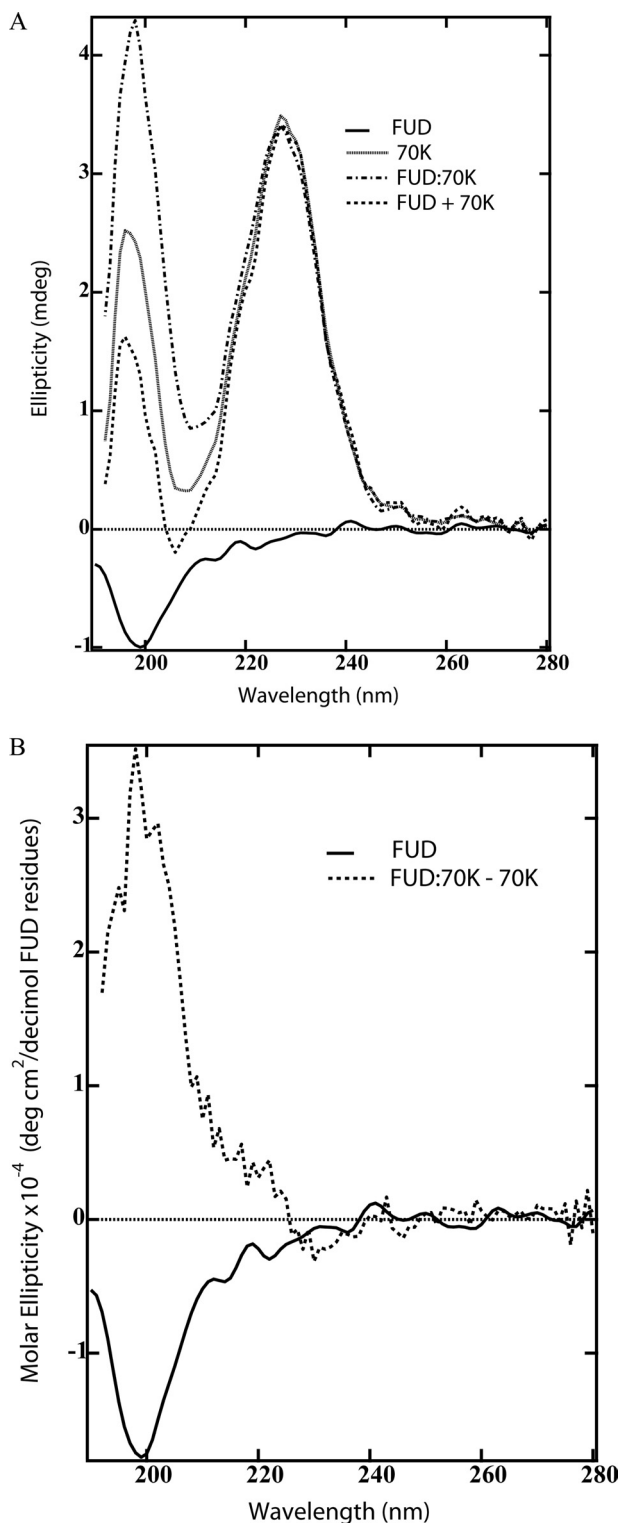


FIGURE 9. Far-UV CD spectra of FUD, 70K, and 70K-FUD complex. A, ellipticities of 1 μ M 70K, FUD, or equimolar 70K-FUD complex were measured from 190 to 280 nm and expressed as millidegrees (mdeg). The solid line, dotted line, dash-dotted line, and dash line represent, respectively, FUD, 70K, FUD-70K complex, and the sum of FUD and 70K (FUD + 70K). B, assuming that the difference between the signals of 70K and the FUD-70K complex was due to FUD alone, the spectrum of 70K was subtracted from the spectrum of the FUD-70K complex to generate the spectrum of FUD after binding. The ellipticities of FUD uncomplexed and complexed FUD are expressed in molar ellipticity $\times 10^{-4}$ using the standard convention of degrees/dmol of amino acid.

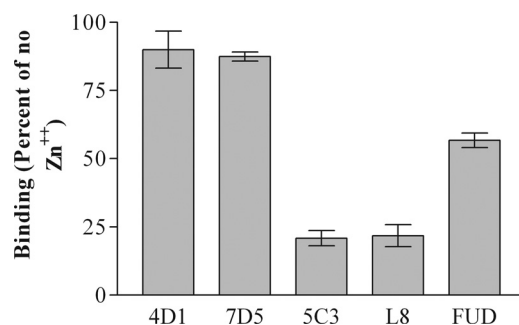


FIGURE 10. Effects of Zn²⁺ on FUD and mAb binding to FN. Binding relative to no Zn²⁺ of 4D1 (1:50,000 ascites), 7D5 (1:50,000 ascites), 5C3 (1:30,000 ascites), L8 (0.1 μ g/ml), or 0.3 nM b-FUD to coated FN. Values are means \pm S.D. of three experiments.

199-nm band of FUD and positive 198-nm band of the difference spectrum are compatible with uncomplexed FUD being largely random coil and complexed FUD being largely in β -sheet (45, 46).

Zn²⁺ Affects FUD Binding to FN—Based on crystallographic and NMR analyses of microbial surface components recognizing adhesive matrix molecule-derived or collagen peptides bound to tandem FNI modules (26–28, 40, 47), one would predict that the increased β -structure arises from FUD binding to C-D-E sheets of consecutive FNI modules by the β -zipper mechanism. A recent crystallographic study showed that 30–50 mM Zn²⁺ dramatically alters the structure of ⁷FNI-⁹FNI such that ⁸FNI loses the canonical FNI fold and instead interacts with ⁷FNI and ⁹FNI by β -strand extensions (48). As would be expected based on this structure, mAbs 5C3 or L8 bound less well to coated FN in the presence of 1 mM Zn²⁺, whereas binding of 4D1 or 7D5 was largely unaffected (Fig. 10). Incubation of 1 mM Zn²⁺ with b-FUD caused a \sim 40% decrease in b-FUD compared with b-FUD binding without Zn²⁺ (Fig. 10). These results provide evidence of the involvement of modules within ⁷FNI-⁹FNI and the β -zipper mechanism in binding of FUD to FN.

Modeling of the Interaction between FUD and FN—Crystal structures are available of STATT and STAFF peptides, based on FNBRs of *S. aureus* FNBPA, binding to ²FNI-³FNI and ⁴FNI-⁵FNI (28). Alignments of FNBR in FUD with the sequences of the FNBRs of FNBPA show conserved residues but, as among the FNBRs in FNBPA that bind FN, with considerable sequence dissimilarity (28, 30). Given this sequence dissimilarity, we used the Sybyl modeling program to learn if it is possible for FUD to bind to ²FNI-³FNI using interactions found in crystal structures of the STATT-5 and STAFF-5 peptides bound, respectively, to ²FNI-³FNI and ⁴FNI-⁵FNI (28). Two approaches were taken. First, we modeled a stretch of FUD binding to the ²FNI-³FNI or ⁴FNI-⁵FNI tandem pairs (Fig. 11, A and B). Second, we compared the energies of 6-residue peptides binding to individual modules (Table 2).

For the interaction with ²FNI, FUD was anchored based on the EDT sequence at the C terminus of FUD that is found in STATT-5 (Fig. 11, A and B). Arg-107 recognized by 4D1 is on the opposite face of ²FNI (Figs. 6C and 11B). Calculations of energies of binding of the 6-residue STATT-5 peptide and residues 43–48 of FUD indicated that both interactions are

FUD Interactions with the N Terminus of Fibronectin

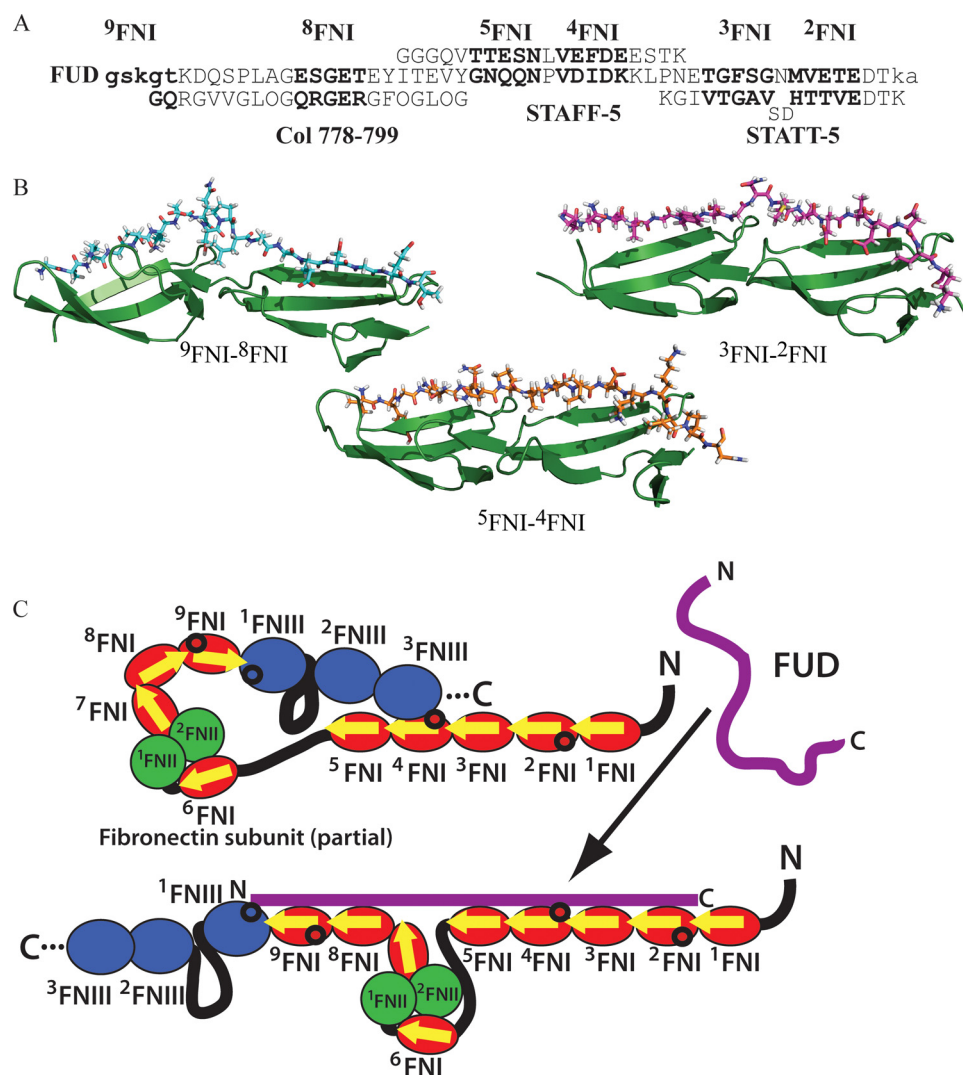


FIGURE 11. Modeling of β -zipper formation between FUD and FN. *A*, alignment of residues of FUD and peptides in crystal structures (28, 40). Residues that participate in the β -sheet interaction in the crystal structures (28, 40) and models are in *boldface*. *B*, homology models of segments of FUD bound to ²FNI-³FNI, ⁴FNI-⁵FNI, or ⁸FNI-⁹FNI. FNI modules are from C to N termini, and FUD sequences are from N to C termini. *C*, models of uncomplexed FN N-terminal modules and changes that accompany complex formation. *Top panel*, FN is shown with ³FNIII folded back to interact with ⁴FNI, and free FUD is shown as a random coil. *Bottom panel*, FUD is shown bound to ²FNI-⁵FNI and ⁸FNI-⁹FNI. *Black circles* show location of mAbs: 4D1 in ²FNI, 7D5 in ⁴FNI, 5C3 in ⁹FNI, and L8 in ¹FNIII. *Yellow arrows* depict the E-strands.

more favorable than binding of a 6-alanine sequence, and indeed the binding of the FUD sequence is more favorable than the binding of the STATT-5 sequence (Table 2). Energies of ³FNI interacting residues 36–41 and 35–40 were determined, with 36–41 forming a complex with the more favorable energy (Table 2). Skipping one residue, instead of two residues seen with FNBPA-5 peptides in the crystal structure (28), before the first backbone hydrogen bond with ³FNI at Gly-41 (Fig. 11, *A* and *B*), places Phe-39 in a hydrophobic rather than a hydrophilic pocket.

In modeling the interaction of FUD with ⁴FNI-⁵FNI, we were directed by the NMR analysis of a complex of a peptide including residues 18–36 of FUD with a tandem ⁴FNI-⁵FNI construct (26). We placed the first backbone hydrogen bond with ⁴FNI at Lys-31 of FUD and the first backbone hydrogen bond with ⁵FNI at Asn-25 of FUD (Fig. 11, *A* and *B*). Compared with the calculated interactions of peptides based on STAFF-5, energies of the complexes of FUD peptides were

worse for ⁴FNI and better for ⁵FNI (Table 2). Thus, modeling suggests that it is possible for residues 21–25, 27–31, 37–41, and 43–47 of FUD to interact by the β -zipper mechanism with ⁵FNI, ⁴FNI, ³FNI, and ²FNI, respectively, in a way that is energetically favorable for each of the interfaces (Fig. 11, *A* and *B*, and Table 2).

To account for the importance of the gelatin-binding domain of FN in the binding of FUD, it has been hypothesized that the nonrepetitive region of FUD interacts with ⁶FNI-⁷FNI (21). Inhibition of binding by mAbs 5C3 or L8 or by inclusion of Zn²⁺ in the assays, however, implicates ⁷FNI-⁹FNI with the canonical folds and head-to-tail arrangement of FNI modules as a binding site for FUD. Thus, we modeled binding of the N-terminal residues of FUD to ⁸FNI and ⁹FNI, using residues from FUD to replace the collagen-derived peptide that interacts with ⁸FNI-⁹FNI in crystals of the peptide in complex with a tandem ⁸FNI-⁹FNI construct (40). Residues 8–13 were predicted to bind

TABLE 2
Energies for homology modeling

Energies in kcal/mol for indicated sequences bound to individual FNI modules are shown. FUD residues are numbered as in Fig. 1C. The sequences with * are those found in the models in Fig. 11B.

Module	Peptide	Sequence	kcal/mol
² FNI	STATT-5	HTTVED	-614
² FNI	FUD(43-48)	MVETED*	-704
² FNI	Alanines	AAAAAA	-498
³ FNI	STATT-5	IVTGAV	-514
³ FNI	FUD(35-40)	NETGFS	-520
³ FNI	FUD(36-41)	ETGFSG*	-571
³ FNI	Alanines	AAAAAA	-509
⁴ FNI	STAFF-5	VEFDEE	-506
⁴ FNI	FUD(27-32)	VDIDKK*	-462
⁴ FNI	Alanines	AAAAAA	-404
⁵ FNI	STAFF-5	VTTESN	-699
⁵ FNI	FUD(20-25)	YGNQQN*	-723
⁵ FNI	Alanines	AAAAAA	-687
⁸ FNI	Collagen	GQRGER	-624
⁸ FNI	FUD(4-9)	SPLAGE	-519
⁸ FNI	FUD(5-10)	PLAGES	-558
⁸ FNI	FUD(6-11)	LAGESG	-499
⁸ FNI	FUD(7-12)	AGESGE	-555
⁸ FNI	FUD(8-13)	GESGET*	-587
⁸ FNI	FUD(9-14)	ESGETE	-557
⁸ FNI	FUD(10-15)	SGETEY	-581
⁸ FNI	FUD(11-16)	GETEYI	-542
⁸ FNI	FUD(12-17)	ETEYIT	-557
⁸ FNI	Alanines	AAAAAA	-492
⁹ FNI	FUD(-5-1)	gskgtK*	-567
⁹ FNI	FUD(-4-2)	skgtKD	-566
⁹ FNI	FUD(-3-3)	kgtKDQ	-548
⁹ FNI	FUD(-2-4)	gtKDQS	-569
⁹ FNI	FUD(-1-5)	tKDQSP	-559
⁹ FNI	FUD(1-6)	KDQSPL	-517
⁹ FNI	Alanines	AAAAAA	-511

to ⁸FNI with the highest energy of any 6-residue sequence between residues 4 and 17 of FUD, although the binding was predicted to be less favorable than binding of GQRGER of the collagen peptide (Table 2). Thus, we placed the first backbone hydrogen bond with ⁸FNI at Thr-13 (Fig. 11, A and B). However, other 6-residue FUD sequences also interacted with favorable predicted energies when modeled as binding to ⁸FNI (Table 2). Similarly, calculated energies show that there are several peptides upstream of the predicted binding site for ⁸FNI that could bind favorably to ⁹FNI (Table 2). These peptides include a variable number of residues in the tail of FUD that was introduced in the cloning strategy. The model shown in Fig. 11, A and B, uses the bridging that was seen with the collagen peptide bound to the ⁸FNI-⁹FNI complex (40). In this model, GSKGT of FUD bound the E-strand of ⁹FNI (Fig. 11, A and B). Gly-567 recognized by 5C3 is within 11 Å of the portion of FUD that bridges ⁸FNI-⁹FNI (Figs. 6C and 11B).

DISCUSSION

FUD is a powerful antagonist of FN assembly and has become a tool to study the role of FN matrix in biological and pathobiological processes, e.g. angiogenesis, vascular remodeling, thrombosis, and deposition of other matrix proteins (49-52). This study expands the knowledge of how FUD binds to FN to have this effect.

Previous ITC studies with the first FNBR from *S. pyogenes* F1 adhesin, which is the same FNBR as is in FUD and

has presumptive binding sites for ²FNI-⁵FNI (Fig. 1B), demonstrated an affinity for the fibrin-binding domain of 170 nM (26). Addition of the nonrepetitive C-terminal sequence that has been shown to interact with ¹FNI increased the affinity for the fibrin-binding domain to 2 nM (26). This affinity plus the energetics of the interaction are similar to the binding constant and energetics of tight binding of FUD to 70K in our ITC analyses. Thus, the N-terminal region of FUD must interact with parts of 70K other than ²FNI-⁵FNI. We present evidence that these sites are likely in ⁸FNI and ⁹FNI.

CD suggests that FUD is in a random coil when free and changes to β -sheet upon interacting with 70K. ITC studies demonstrating that both enthalpy and entropy decrease in the interaction between FUD and FN or 70K are compatible with formation of hydrogen bonds upon binding. Although we cannot exclude a contribution of a conformational change in 70K to the CD difference spectrum, in crystallography studies (28, 40) unligated and ligated FNI modules in the unit cells had similar structures. Furthermore, the secondary structure and positions of the conserved tyrosines and tryptophans are similar from one FNI module to another FNI module when examined in solution (53, 54) or in crystals (28, 40, 47, 54). Thus, it is reasonable to attribute the difference of spectrum to a major conformational change in FUD without hypothesizing additional changes in the global folds of FNI modules.

The increase rather than decrease in 4D1 binding in the presence of FUD suggests that the FUD-70K β -zipper includes ²FNI and perturbs the 4D1 epitope on the opposite face of the module. 7D5, which recognizes an epitope at the beginning of the E-strand of ⁴FNI, inhibited FUD binding strongly and in turn was inhibited by FUD. Working from structures of parts of FNBRs of *S. aureus* FnBPA in complex with tandem FNI modules (28), we constructed possible models of β -zipper interactions between residues 21 and 47 of FUD and the E-strands of ²FNI-⁵FNI (Fig. 11).

Inhibition of binding with mAbs to ⁹FNI and ¹FNI and the effect of Zn²⁺ on both mAb and FUD binding implicate this region rather than the N-terminal portion of the gelatin-binding region in the FUD-FN interaction. Using homology modeling, we found sites in FUD that could bind favorably to both ⁸FNI and ⁹FNI. However, there are only seven residues between the presumptive binding sites on FUD for ⁵FNI and ⁸FNI (Fig. 11A). Therefore, one must propose a conformation of FN in which the ⁶FNI-⁷FNI complex is not colinear with ⁸FNI-⁹FNI but rather part of a loop that allows ⁵FNI to be close to ⁸FNI (Fig. 11C). NMR and crystallographic studies of ⁶FNI-²FNI and ⁶FNI-⁷FNI (55-57) demonstrated interactions between ⁶FNI and ²FNI, ¹FNI and ²FNI, and ⁷FNI with both ¹FNI and ²FNI, allowing this region of FN to form a complex that has the potential to loop out. The 32-residue stretch of presumably unstructured sequence between ⁵FNI and ⁶FNI likely provides the flexibility to bring ⁵FNI in proximity to ⁸FNI (Fig. 11C). A collagen peptide bound to a linear binding pocket that included ²FNI and ⁷FNI, and it has been suggested that this pocket is part of a larger collagen-binding site that includes ⁸FNI (55). One consequence of this sugges-

tion is that FUD and collagen peptides cross-compete, and indeed we find that gelatin competes for binding of FUD to FN.⁴

Inhibition of b-FUD binding to FN by 5C3 and modeling suggests that the β -zipper extends to occupy the E-strand of ⁹FNI, which may be occupied by the N-terminal tail residues introduced into FUD by the expression strategy. This scheme leaves no residues to interact with ¹FNIII. Inhibition of b-FUD binding to FN with L8 to Gln-690 in ¹FNIII (Fig. 6E) is likely related by the fact that the L8 epitope requires both ⁹FNI and ¹FNIII (36). Alternatively, the part of FUD that interacts with ⁹FNI may be more C-terminal than shown in Fig. 11A, which would provide N-terminal residues that could interact with ¹FNIII. Utilization of residues introduced by the cloning strategy offers an explanation for why the pUR4 FUD construct with an N-terminal tail binds to the gelatin-binding fragment of FN, whereas synthetic FUD lacking the tail does not bind (18). It also supports the notion that the functional upstream domain of the F1 adhesin and BBK32 extends six residues further upstream than in our construct (31). We emphasize, however, that modeling of the interactions between FUD and ⁸FNI-⁹FNI is highly speculative as compared with the modeling of the interaction between FUD and ²FNI-⁵FNI. We were not guided by a consensus sequence with which to anchor FUD on ⁸FNI, a complete structure on which to base the connector linking the FUD sequences interacting with ⁸FNI and ⁹FNI, and knowledge about lability of the tilt and rotation between ⁸FNI and ⁹FNI or how the interaction with ¹FNIII impacts the structure of ⁹FNI.

Both enzyme-linked assays and ITC experiments demonstrated increased affinity of FUD for 70K as compared with FN. The epitope for 7D5 is in close proximity to Arg-222 that contributes to an interaction between isolated ³FNIII and a tandem ⁴FNI-⁵FNI construct that was demonstrated by NMR (58). Although this interaction is weak, evidence for such an intramolecular interaction in FN (Fig. 11C) was corroborated by analysis of the structural determinants of migration stimulating activity (58). Arg-222 is in the E-strand of ⁴FNI, so for FUD to bind to ⁴FNI by the β -zipper mechanism, the ³FNIII-⁴FNI interaction must be broken (Figs. 6C and 11B). The lower free energy of binding of FUD to FN than to 70K is presumably because of coupling of energetically favorable binding via the β -zipper hydrogen bonds to FNI modules to energetically unfavorable conformational changes in FN that include mobilization of ³FNIII away from ⁴FNI (Fig. 11C).

Binding of FUD to FN exposes an epitope for the mAbIII10 antibody in ¹⁰FNIII that includes the RGD cell adhesive sequence (37). The conformational changes induced by FUD therefore may be more profound than breakage of the ³FNIII-⁴FNI interaction. Some of the changes may be linked to changes in ¹FNIII. The ¹FNIII module interacts strongly with ⁹FNI as evidenced by the requirement that ⁹FNI must be folded and contiguous to ¹FNIII for the L8 epitope to be expressed (36). The possibility of the binding of FUD perturbing ¹FNIII is interesting because ¹FNIII interacts with ²FNIII in

such a way that a stretch of 29 residues between the G-strand of ¹FNIII and the B-strand of ²FNIII is flexible (59). Furthermore, ¹FNIII and ²FNIII interact by a salt bridge that can be disrupted easily (59, 60). One can imagine a scenario in which perturbing the ⁹FNI-¹FNIII pair would change the relationship of ¹FNIII with ²FNIII and result in conformational changes that are propagated to perturb interactions among more C-terminal modules (61).

Most of the attention on the interaction between the 70K region and the cell surface to allow FN assembly has focused on integrins. For instance, it has been suggested that spontaneous conversion of NGR sequences in ⁵FNI and ⁷FNI of 70K to integrin binding *iso*-DGR sequences is responsible for the binding of 70K to the cell surface (62–64). However, mutagenesis to prevent isomerization demonstrated that this conversion is dispensable for FN assembly and 70K binding (65). There are also IGD sequences in ³FNI, ⁵FNI, ⁷FNI, and ⁹FNI that stimulate fibroblast migration, a process that involves $\alpha\beta 3$ (66–68). We have found that 70K with mutations in four IGD sequences also do not cause loss of binding to FN assembly sites.⁴ Here, we demonstrate similarities between FUD binding to FN and FN assembly. Specifically, antibodies or FUD mutants that block FUD binding also block FN assembly. Furthermore, 70K is more potent than 27K or 40K for inhibiting both FUD binding to FN and FN assembly (12, 18). These parallels suggest an alternative paradigm in which cell surface molecules catalyze FN assembly by interacting with common features of the tandem FNI modules in 70K rather than discrete sites on certain modules.

Unstructured regions of proteins are biologically important for regulatory and assembly processes (69). Cross-linking of 70K bound to assembly sites is to molecules that either are very large or do not dissociate in SDS, even after reduction (70). We hypothesize that these unidentified targets on the cell surface are unstructured and bind FN via the β -strand addition mechanism that has been subverted by bacteria as exemplified by *S. pyogenes* F1 adhesin and other adhesins. For processes, including both bacterial invasion (71, 72) and FN assembly (6), this binding would expose the integrin-binding RGD motif in FN (37, 73) and allow integrins to engage FN.

REFERENCES

- George, E. L., Georges-Labouesse, E. N., Patel-King, R. S., Rayburn, H., and Hynes, R. O. (1993) *Development* **119**, 1079–1091
- Dzamba, B. J., Jakab, K. R., Marsden, M., Schwartz, M. A., and DeSimone, D. W. (2009) *Dev. Cell* **16**, 421–432
- Sakai, T., Johnson, K. J., Murozono, M., Sakai, K., Magnuson, M. A., Wieloch, T., Cronberg, T., Isshiki, A., Erickson, H. P., and Fässler, R. (2001) *Nat. Med.* **7**, 324–330
- Cho, J., and Mosher, D. F. (2006) *J. Thromb. Haemost.* **4**, 1461–1469
- Maurer, L. M., Tomasini-Johansson, B. R., and Mosher, D. F. (2010) *Thromb. Res.* **125**, 287–291
- Geiger, B., Bershadsky, A., Pankov, R., and Yamada, K. M. (2001) *Nat. Rev. Mol. Cell Biol.* **2**, 793–805
- Mao, Y., and Schwarzbauer, J. E. (2005) *Matrix Biol.* **24**, 389–399
- Tomasini-Johansson, B. R., Annis, D. S., and Mosher, D. F. (2006) *Matrix Biol.* **25**, 282–293
- Mosher, D. F. (1993) *Curr. Opin. Struct. Biol.* **3**, 214–222
- Tucker, R. P., and Chiquet-Ehrismann, R. (2009) *Int. J. Biochem. Cell Biol.* **41**, 424–434
- Maas, C., Schiks, B., Strangi, R. D., Hackeng, T. M., Bouma, B. N., Geb-

⁴ L. M. Maurer and D. F. Mosher, unpublished data.

- bink, M. F., and Bouma, B. (2008) *Amyloid*. **15**, 166–180
12. McKeown-Longo, P. J., and Mosher, D. F. (1985) *J. Cell Biol.* **100**, 364–374
 13. Cho, J., and Mosher, D. F. (2006) *J. Thromb. Haemost.* **4**, 943–951
 14. Dzamba, B. J., Bultmann, H., Akiyama, S. K., and Peters, D. M. (1994) *J. Biol. Chem.* **269**, 19646–19652
 15. Sechler, J. L., Takada, Y., and Schwarzbauer, J. E. (1996) *J. Cell Biol.* **134**, 573–583
 16. Bultmann, H., Santas, A. J., and Peters, D. M. (1998) *J. Biol. Chem.* **273**, 2601–2609
 17. Sottile, J., Schwarzbauer, J., Selegue, J., and Mosher, D. F. (1991) *J. Biol. Chem.* **266**, 12840–12843
 18. Ensenberger, M. G., Tomasini-Johansson, B. R., Sottile, J., Ozeri, V., Hanski, E., and Mosher, D. F. (2001) *J. Biol. Chem.* **276**, 35606–35613
 19. Tomasini-Johansson, B. R., Kaufman, N. R., Ensenberger, M. G., Ozeri, V., Hanski, E., and Mosher, D. F. (2001) *J. Biol. Chem.* **276**, 23430–23439
 20. Schwarz-Linek, U., Höök, M., and Potts, J. R. (2004) *Mol. Microbiol.* **52**, 631–641
 21. Schwarz-Linek, U., Höök, M., and Potts, J. R. (2006) *Microbes Infect.* **8**, 2291–2298
 22. Ozeri, V., Tovi, A., Burstein, I., Natanson-Yaron, S., Caparon, M. G., Yamada, K. M., Akiyama, S. K., Vlodavsky, I., and Hanski, E. (1996) *EMBO J.* **15**, 989–998
 23. Talay, S. R., Zock, A., Rohde, M., Molinari, G., Oggioni, M., Pozzi, G., Guzman, C. A., and Chhatwal, G. S. (2000) *Cell Microbiol.* **2**, 521–535
 24. House-Pompeo, K., Xu, Y., Joh, D., Speziale, P., and Höök, M. (1996) *J. Biol. Chem.* **271**, 1379–1384
 25. Kim, J. H., Singvall, J., Schwarz-Linek, U., Johnson, B. J., Potts, J. R., and Höök, M. (2004) *J. Biol. Chem.* **279**, 41706–41714
 26. Schwarz-Linek, U., Pilka, E. S., Pickford, A. R., Kim, J. H., Höök, M., Campbell, I. D., and Potts, J. R. (2004) *J. Biol. Chem.* **279**, 39017–39025
 27. Schwarz-Linek, U., Werner, J. M., Pickford, A. R., Gurusiddappa, S., Kim, J. H., Pilka, E. S., Briggs, J. A., Gough, T. S., Höök, M., Campbell, I. D., and Potts, J. R. (2003) *Nature* **423**, 177–181
 28. Bingham, R. J., Rudiño-Piñera, E., Meenan, N. A., Schwarz-Linek, U., Turkenburg, J. P., Höök, M., Garman, E. F., and Potts, J. R. (2008) *Proc. Natl. Acad. Sci. U.S.A.* **105**, 12254–12258
 29. Lin, Y. P., Greenwood, A., Nicholson, L. K., Sharma, Y., McDonough, S. P., and Chang, Y. F. (2009) *J. Biol. Chem.* **284**, 23547–23557
 30. Meenan, N. A., Visai, L., Valtulina, V., Schwarz-Linek, U., Norris, N. C., Gurusiddappa, S., Höök, M., Speziale, P., and Potts, J. R. (2007) *J. Biol. Chem.* **282**, 25893–25902
 31. Raibaud, S., Schwarz-Linek, U., Kim, J. H., Jenkins, H. T., Baines, E. R., Gurusiddappa, S., Höök, M., and Potts, J. R. (2005) *J. Biol. Chem.* **280**, 18803–18809
 32. Mosher, D. F., and Johnson, R. B. (1983) *J. Biol. Chem.* **258**, 6595–6601
 33. Mosher, D. F., Huwiler, K. G., Misenheimer, T. M., and Annis, D. S. (2002) *Methods Cell Biol.* **69**, 69–81
 34. Xu, J., Bae, E., Zhang, Q., Annis, D. S., Erickson, H. P., and Mosher, D. F. (2009) *PLoS One*. **4**, e4113
 35. Sottile, J., Selegue, J., and Mosher, D. F. (1990) *Protein Expr. Purif.* **1**, 104–110
 36. Chernousov, M. A., Fogerty, F. J., Kotliansky, V. E., and Mosher, D. F. (1991) *J. Biol. Chem.* **266**, 10851–10858
 37. Ensenberger, M. G., Annis, D. S., and Mosher, D. F. (2004) *Biophys. Chem.* **112**, 201–207
 38. Saoncella, S., Echtermeyer, F., Denhez, F., Nowlen, J. K., Mosher, D. F., Robinson, S. D., Hynes, R. O., and Goetinck, P. F. (1999) *Proc. Natl. Acad. Sci. U.S.A.* **96**, 2805–2810
 39. Annis, D. S., Murphy-Ullrich, J. E., and Mosher, D. F. (2006) *J. Thromb. Haemost.* **4**, 459–468
 40. Erat, M. C., Slatte, D. A., Lowe, E. D., Millard, C. J., Farndale, R. W., Campbell, I. D., and Vakonakis, I. (2009) *Proc. Natl. Acad. Sci. U.S.A.* **106**, 4195–4200
 41. Powell, M. (1977) *Math. Program.* **12**, 241–254
 42. Beychok, S. (1966) *Science* **154**, 1288–1299
 43. Odermatt, E., and Engel, J. (1989) in *Biology of Extracellular Matrix* (Mosher, D. F., ed) pp. 29–45, Academic Press, Inc., San Diego
 44. Greenfield, N., and Fasman, G. D. (1969) *Biochemistry* **8**, 4108–4116
 45. Kelly, S. M., Jess, T. J., and Price, N. C. (2005) *Biochim. Biophys. Acta* **1751**, 119–139
 46. Greenfield, N. J. (1996) *Anal. Biochem.* **235**, 1–10
 47. Rudiño-Piñera, E., Ravelli, R. B., Sheldrick, G. M., Nanao, M. H., Korostelev, V. V., Werner, J. M., Schwarz-Linek, U., Potts, J. R., and Garman, E. F. (2007) *J. Mol. Biol.* **368**, 833–844
 48. Graille, M., Pagano, M., Rose, T., Ravaux, M. R., and van Tilbeurgh, H. (2010) *Structure* **18**, 710–718
 49. Chiang, H. Y., Korshunov, V. A., Serour, A., Shi, F., and Sottile, J. (2009) *Arterioscler. Thromb. Vasc. Biol.* **29**, 1074–1079
 50. Zhou, X., Rowe, R. G., Hiraoka, N., George, J. P., Wirtz, D., Mosher, D. F., Virtanen, I., Chernousov, M. A., and Weiss, S. J. (2008) *Genes Dev.* **22**, 1231–1243
 51. Cho, J., and Mosher, D. F. (2006) *Blood* **107**, 3555–3563
 52. Sabatier, L., Chen, D., Fagotto-Kaufmann, C., Hubmacher, D., McKee, M. D., Annis, D. S., Mosher, D. F., and Reinhardt, D. P. (2009) *Mol. Biol. Cell* **20**, 846–858
 53. Baron, M., Norman, D., Willis, A., and Campbell, I. D. (1990) *Nature* **345**, 642–646
 54. Williams, M. J., Phan, I., Harvey, T. S., Rostagno, A., Gold, L. L., and Campbell, I. D. (1994) *J. Mol. Biol.* **235**, 1302–1311
 55. Erat, M. C., Schwarz-Linek, U., Pickford, A. R., Farndale, R. W., Campbell, I. D., and Vakonakis, I. (2010) *J. Biol. Chem.* **285**, 33764–33770
 56. Pagett, A., Campbell, I. D., and Pickford, A. R. (2005) *Biochemistry* **44**, 14682–14687
 57. Pickford, A. R., Smith, S. P., Staunton, D., Boyd, J., and Campbell, I. D. (2001) *EMBO J.* **20**, 1519–1529
 58. Vakonakis, I., Staunton, D., Ellis, I. R., Sarkies, P., Flanagan, A., Schor, A. M., Schor, S. L., and Campbell, I. D. (2009) *J. Biol. Chem.* **284**, 15668–15675
 59. Vakonakis, I., Staunton, D., Rooney, L. M., and Campbell, I. D. (2007) *EMBO J.* **26**, 2575–2583
 60. Karuri, N. W., Lin, Z., Rye, H. S., and Schwarzbauer, J. E. (2009) *J. Biol. Chem.* **284**, 3445–3452
 61. Johnson, K. J., Sage, H., Briscoe, G., and Erickson, H. P. (1999) *J. Biol. Chem.* **274**, 15473–15479
 62. Corti, A., Curnis, F., Arap, W., and Pasqualini, R. (2008) *Blood* **112**, 2628–2635
 63. Curnis, F., Longhi, R., Crippa, L., Cattaneo, A., Dondossola, E., Bachi, A., and Corti, A. (2006) *J. Biol. Chem.* **281**, 36466–36476
 64. Takahashi, S., Leiss, M., Moser, M., Ohashi, T., Kitao, T., Heckmann, D., Pfeifer, A., Kessler, H., Takagi, J., Erickson, H. P., and Fässler, R. (2007) *J. Cell Biol.* **178**, 167–178
 65. Xu, J., Maurer, L. M., Hoffmann, B. R., Annis, D. S., and Mosher, D. F. (2010) *J. Biol. Chem.* **285**, 8563–8571
 66. Ellis, I. R., Jones, S. J., Staunton, D., Vakonakis, I., Norman, D. G., Potts, J. R., Milner, C. M., Meenan, N. A., Raibaud, S., Ohea, G., Schor, A. M., and Schor, S. L. (2010) *Exp. Cell Res.* **316**, 2465–2476
 67. Millard, C. J., Ellis, I. R., Pickford, A. R., Schor, A. M., Schor, S. L., and Campbell, I. D. (2007) *J. Biol. Chem.* **282**, 35530–35535
 68. Schor, S. L., Ellis, I., Banyard, J., and Schor, A. M. (1999) *J. Cell Sci.* **112**, 3879–3888
 69. Wright, P. E., and Dyson, H. J. (1999) *J. Mol. Biol.* **293**, 321–331
 70. Zhang, Q., and Mosher, D. F. (1996) *J. Biol. Chem.* **271**, 33284–33292
 71. Ozeri, V., Rosenshine, I., Ben-Ze'Ev, A., Bokoch, G. M., Jou, T. S., and Hanski, E. (2001) *Mol. Microbiol.* **41**, 561–573
 72. Ozeri, V., Rosenshine, I., Mosher, D. F., Fässler, R., and Hanski, E. (1998) *Mol. Microbiol.* **30**, 625–637
 73. Ugarova, T. P., Zamarron, C., Veklich, Y., Bowditch, R. D., Ginsberg, M. H., Weisel, J. W., and Plow, E. F. (1995) *Biochemistry* **34**, 4457–4466